AIP | Journal of Applied Physics

Temperature and pressure effects of multiferroic Bi2NiTiO6 compound

Jinlong Zhu, Shaomin Feng, Qingqing Liu, Jianzhong Zhang, Hongwu Xu et al.

Citation: J. Appl. Phys. **113**, 143514 (2013); doi: 10.1063/1.4801630
View online: http://dx.doi.org/10.1063/1.4801630
View Table of Contents: http://jap.aip.org/resource/1/JAPIAU/v113/i14
Published by the American Institute of Physics.

Temperature and pressure effects of multiferroic Bi_2NiTiO_6 compound

Jinlong Zhu,[1,2] Shaomin Feng,[1] Qingqing Liu,[1] Jianzhong Zhang,[2,a)] Hongwu Xu,[3] Yanchun Li,[4] Xiaodong Li,[4] Jing Liu,[4] Qingzhen Huang,[5] Yusheng Zhao,[1,2,6,a)] and Changqing Jin[1,a)]

[1]*National Lab for Condensed Matter Physics, Institute of Physics, Chinese Academy of Sciences, Beijing 100190, China*
[2]*LANSCE, Los Alamos National Laboratory, Los Alamos, New Mexico 87545, USA*
[3]*EES Division, Los Alamos National Laboratory, Los Alamos, New Mexico 87545, USA*
[4]*Institute of High Energy Physics, Beijing High Pressure Research Center, Chinese Academy of Sciences, Beijing 100039, People's Republic of China*
[5]*NIST Center for Neutron Research, Notional Institute of Standards and Technology, Gaithersburg, Maryland 20899-6102, USA*
[6]*HiPSEC, Department of Physics and Astronomy, University of Nevada, Las Vegas, Nevada 89154, USA*

(Received 1 February 2013; accepted 27 March 2013; published online 12 April 2013)

Bi_2NiTiO_6 compound which shows both magnetic ($T_M = 58$ K) and ferroelectric properties ($T_C = 513$ K) was synthesized under high pressure of 5 GPa and temperature of 1273 K. The crystal structure, as determined by X-ray powder diffraction and neutron powder diffraction, is a distorted $A(B_1B_2)O_3$ type perovskite with space group $Pn2_1a$. Structural evolution of multiferroic Bi_2NiTiO_6 shows that there are two isostructural phase transitions at ~2 GPa and ~15 GPa under high pressure and at room temperature and indicates that isostructural phase transitions occurred with temperature higher than 823 K under ambient condition. All the isostructural phase transitions come from the Bi ion discontinuous shift, which identifies the phase transition at ~15 GPa and at temperature higher than 823 K are the same. Using a modified high-T Birch-Murnaghan equation of state and a thermal-pressure approach, we have derived the thermoelastic parameters of high pressure phase Bi_2NiTiO_6, including the ambient bulk modulus K_0, temperature derivative of bulk modulus at constant pressure, volumetric thermal expansivity, pressure derivative of thermal expansion, and temperature derivative of bulk modulus at constant volume. © *2013 AIP Publishing LLC* [http://dx.doi.org/10.1063/1.4801630]

I. INTRODUCTION

Multiferroic compounds with coexisting magnetic and ferroelectric orders and magnetoelectric interaction are a class of electronic functional materials. Such materials are highly interesting from both fundamental and technological points of view. Although early attempts to combine ferromagnetic and ferroelectric ordering states in a single material can be traced back to 1960s,[1,2] the research has not received growing attention until 2000s while strong magnetic and electric coupling was observed in transition metal oxides.[3,4] Ferroelectricity and ferromagnetism usually exclude each other.[5,6] To polarize a crystal, the structure needs to be non-centrosymmetric such that it prefers non-magnetic ions. On the other hand, ferromagnetism is commonly occurs in materials containing transition metal ions with unpaired outer shell electrons. As a result, single-phase multiferroic compounds are to date quite scarce. Bi- and Pb-based ferroelectric compounds have received much attention in recent years due to their superior properties for technological applications.[3,4,7,8] It is believed that the spontaneous polarization in these compounds mainly results from the ns^2 lone pair. As it has been reported by Azuma *et al.*,[7] a classical way to obtain multiferroic properties in ABO_3 system is to have Bi^{3+} and Pb^{2+} at A site and magnetic transition metal ions at B site. Until now, the most studied Bi-based multiferroic perovskites are $BiMnO_3$ [Refs. 9–15] and $BiFeO_3$ [Refs. 16 and 17] with magnetic Mn or Fe ions at B site. However, those compounds usually show large leakage current partially caused by the presence of d electrons, which leads to high density of states near the Fermi surface and improved conductivity with narrow band gaps. $BaTiO_3$ represents another type of classic ferroelectric compound in which the covalent bonding between non-magnetic Ti^{4+} and O^{2-} enhances the spontaneous polarization.[18] Therefore, a common strategy to formulate new multiferroic compounds is to incorporate both magnetic and non-magnetic ions at B sites in favor of ferroelectricity.

Here we report the multiferroic compound Bi_2NiTiO_6, which has been studied as ferroelectric materials recently,[19–21] has successfully been synthesized by means of high pressure sintering. The crystal structure, as determined by powder X-ray and neutron diffraction methods, is a La_2CuTiO_6-type[22] double perovskite with non-centrosymmetric space group $Pn2_1a$. We studied structural stability and equation of state of this multiferroic compound by synchrotron X-ray diffraction at elevated pressures and temperatures.

II. EXPERIMENTAL SECTION

The bulk sample of Bi_2NiTiO_6 was prepared at 5 GPa in a cubic anvil-type high-pressure apparatus at 1273 K for 30 min. The powder X-ray diffraction (XRD) experiments at ambient conditions were performed with an M18AHF

[a)]Authors to whom correspondence should be addressed. Electronic addresses: jzhang@lanl.gov; Yusheng.Zhao@unlv.edu; and Jin@iphy.ac.cn.

diffractometer (MAC SCIENCE, Japan) employing Cu $K\alpha_1$ radiation in a step scanning mode (3 s counting time for $\Delta 2\theta = 0.02°$). The neutron powder diffraction was performed at the Center for Neutron Research, Notional Institute of Standards and Technology, Gaithersburg, Maryland with a wavelength $\lambda = 1.5403$ Å. Magnetic susceptibility was measured with a superconducting quantum interference device (SQUID) magnetometer (Quantum Design MPMS XL) in magnetic fields of 100 Oe, 1000 Oe, 1 T, 3 T, 5 T, and 7 T. Dielectric constant measurement was carried out by an HP4294A impedance analyzer at temperatures between 300 K and 600 K. High-pressure synchrotron angle-dispersive X-ray diffraction (AD-XRD) experiment was performed at room temperature at 3W1A high-pressure beam-line of Beijing Synchrotron Radiation Facility (BSRF), with a wavelength of 0.6199. The sample was loaded into the sample chamber in a T301 stainless steel gasket. The pressure was measured by using the ruby fluorescence method.[23] A mixture of methanol and ethanol (4:1) was used as pressure-transmitting medium. XRD diffraction at elevated temperature was performed in an X' Pert PRO X-ray diffractometer employing an HTK16 high-temperature stage and Cu $K\alpha_1$ radiation. High *P-T* synchrotron XRD experiments were performed using a cubic anvil apparatus at beamline X17B2 of the National Synchrotron Light Source (NSLS), Brookhaven National Laboratory. The white radiation from the superconducting wiggler magnet was used for energy-dispersive measurements. The diffracted X-rays were collected with a multi-element detector at a fixed Bragg angle of $2\theta = 6.250°$. The cell assembly used has been described in detail elsewhere.[24] Briefly, a cube made up of a mixture of amorphous boron and epoxy resin was employed as pressure-transmitting medium, and amorphous carbon was used as furnace material to achieve high temperature. The Bi_2NiTiO_6 and NaCl powders (used as the pressure marker) were packed into separate layers in a cylindrical boron nitride (BN) container of 1.0 mm diameter and 2.0 mm length. Data were collected on both Bi_2NiTiO_6 and NaCl at each experimental condition. The relative standard deviations in the determined unit-cell volumes are typically less than 0.1%. Data processing and structure refinement were performed using the GSAS program package.[25]

III. RESULTS AND DISCUSSION

A. Multi-scale characterization of as-prepared sample

The Bi_2NiTiO_6 sample recovered from high *P-T* synthesis is fully dense and well crystallized with a grain size of several microns, as revealed by scanning electron microscope (SEM) observations. Energy dispersive X-ray spectroscopy (EDX) measurement on a single grain of as-prepared sample shows atomic ratios of Bi:Ti:Ni: O = 2:0.9:1.1:6.1. Within the error of EDX analysis, our sample has the ideal composition of Bi_2NiTiO_6. These combined properties indicate that the as-prepared sample is a good candidate for ferroelectric property measurement.

Figure 1(a) shows the XRD pattern collected for Bi_2NiTiO_6 at room temperature. All reflections can well be indexed to an orthorhombic structure with space group $Pn2_1a$.

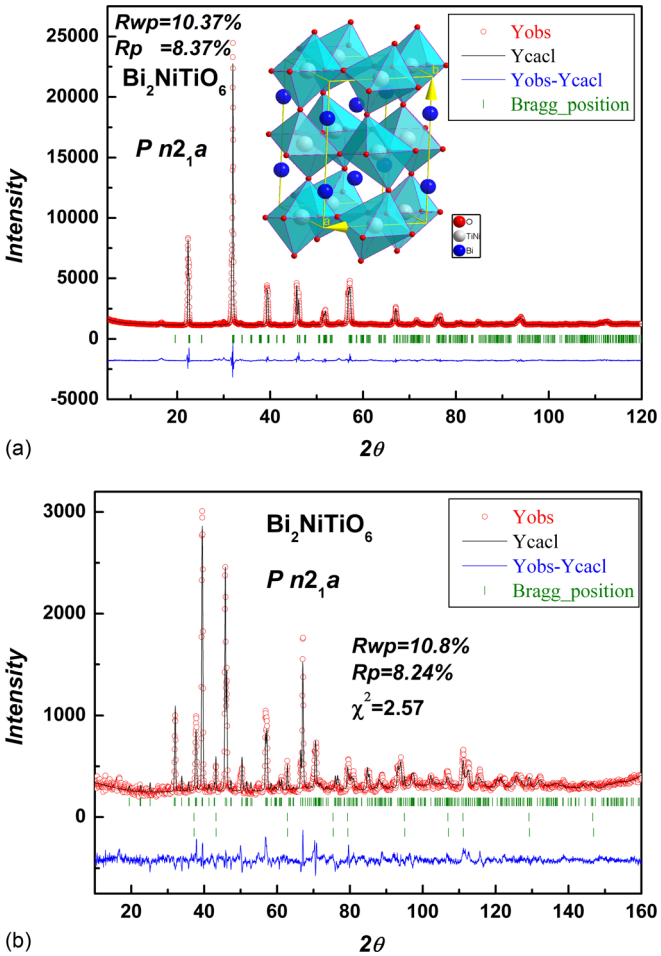

FIG. 1. (a) The observed (crosses), calculated (solid line), and difference patterns resulting from the Rietveld analysis of the X-ray powder diffraction data for Bi_2NiTiO_6 at room temperature in space group $Pn2_1a$. Bragg reflections are indicated by tick marks. Inset shows the simulated crystal structure of Bi_2NiTiO_6. (b) The refined data of neutron diffraction pattern. The impurities are NiO and TiO, respectively. Final fractional coordinates and thermal parameters are listed in Table I.

The final *R* factors of the refinement are Rwp = 10.37% and Rp = 8.37%. Inset of Figure 1(a) shows the simulated crystal structure. Note that $Pn2_1a$ is a subgroup of *Pnma*.[19] To further resolve this distinction, we collected neutron powder diffraction data on the same specimen, as shown Figure 1(b), which are more sensitive than XRD to the atomic positions of oxygen in crystal structure. The refinement with space group $Pn2_1a$ gives Rwp = 10.8%, Rp = 8.24%, and $\chi^2 = 2.57$. The refined lattice parameters are $a = 5.61(\pm 0.01)$ Å, $b = 7.85(\pm 0.01)$ Å, and $c = 5.58(\pm 0.01)$ Å. The site occupancies of Ti and Ni cations were also refined. The site occupancies of Bi cation and O anions are slight off the ideal 1 (less than 1%) and therefore fixed during the refinement. The impurity phases NiO and TiO were also refined in the neutron diffraction data. The fractional coordinates, site occupancies, and thermal parameters (U_{iso}) as well as the fractions of impurity phases from the refinement of neutron diffraction data are listed in Table I. It can be seen that Bi, Ni, and Ti ions all shift away from the positions of (0, 0.25, 0), (0, 0, 0.5), and (0, 0, 0.5) in *Pnma* space group. Alternatively, when we refine the diffraction data with *Pnma*, the thermal parameters for Bi are

TABLE I. Refined fractional coordinates, occupation, and thermal parameters *Uiso* as well as the fractions of impurity phases of NiO and TiO from neutron diffraction data.

	Coordinates of equivalent positions				
Atom type	x	y	z	Occupancy	Uiso
Bi	0.004123	0.254732	0.040243	1.00	0.0448
Ni	−0.021091	−0.000450	0.502552	0.4734	0.0016
Ti	−0.059483	0.009863	0.526880	0.5266	0.0016
O(1)	0.559464	0.251153	−0.035540	1.00	0.0648
O(2)	0.281899	−0.005499	0.270987	1.00	0.0791
O(3)	0.742255	0.054996	0.739912	1.00	0.0798
	Phase fractions				
Bi_2NiTiO_6 95(2) mol. %		TiO 1.4(1) mol. %		NiO 3.6(3) mol. %	

nonisotropic with an abnormally large U_{11} value, suggesting that Bi ion shifts away from the ideal position in *Pnma* group. Because Bi_2NiTiO_6 is ferroelectric,[20] another argument that favors $Pn2_1a$ is that this space group does not possess a center of symmetry whereas *Pnma* is centrosymmetric and thus intrinsically prohibits ferroelectricity.

Figure 2 shows dielectric constant and dielectric loss ($\tan\delta$) measured at a frequency of 100 kHz. Dielectric anomalies with significant hysteresis between heating and cooling cycles are clearly revealed, indicating a classical, first-ordered ferroelectric phase transition at a temperature around $T_C = 513$ K. Figure 3(a) displays zero-field-cooled (ZFC) and field-cooled (FC) magnetic susceptibilities of Bi_2NiTiO_6 measured at $H = 100$ Oe and T = 5–300 K. The ZFC and FC susceptibility curves start splitting below 60 K, with the ZFC susceptibility peaked at $T_M = 58$ K. The inverse ZFC susceptibilities are displayed in the inset of Figure 3(a), including a Curie-Weiss law fitting, $\chi = C/(T - T_\theta)$, of the data above 165 K. The values of Curie-Weiss temperature T_θ and effective magnetic moment μ_{eff} are −242.7 K and 2.28 μB/f.u., which reflect a strong antiferromagnetic interaction and magnetic frustration in this system. With increasing magnetic field, the anomalies are strongly depressed at

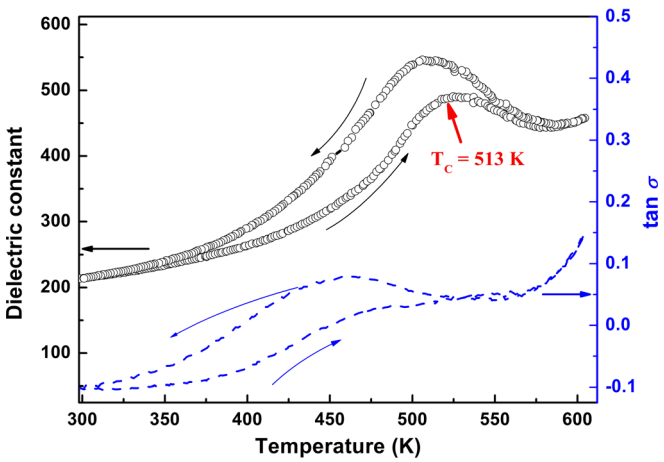

FIG. 2. Dielectric constant and dielectric loss (tan δ) measured at 100 kHz as a function of temperature from 300 K to 600 K under ambient condition.

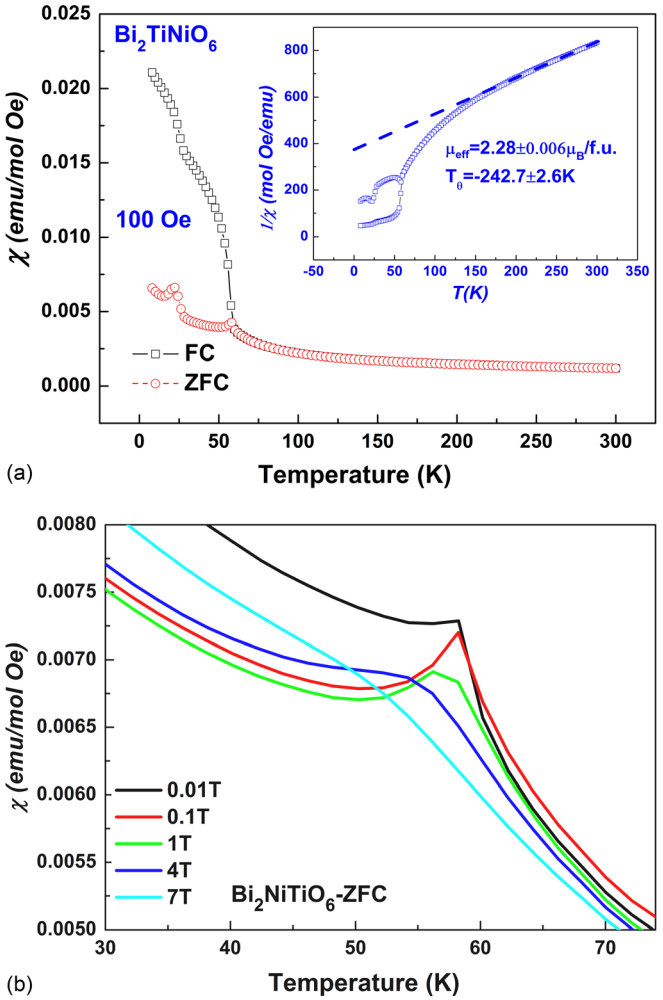

FIG. 3. (a) ZFC and FC magnetic susceptibilities of Bi_2NiTiO_6. The inset shows the inverse susceptibility χ^{-1} (T) of FC and ZFC measurements, with a Curie-Weiss law fit above 165 K. (b) The ZFC magnetic susceptibilities of Bi_2NiTiO_6 under different magnetic field up to 7 T.

$H = 7$ T, indicating a ferromagnetic-like, probably short ranged, magnetic contribution to the magnetization behavior, as shown in Figure 3(b). So in this Bi_2NiTiO_6 system, the magnetic interaction is complicated, showing a canted spin interaction and an inhomogeneous magnetic state.

B. Structure stability of multiferroic compound Bi_2NiTiO_6 under high pressure and temperature

Figure 4(a) shows a representative refined diffraction pattern at 8.43 GPa, and Fig. 4(b) shows all XRD patterns collected at room temperature from ambient pressure to 36.7 GPa. Evidently, when pressure is higher than 2 GPa, a number of new diffraction peaks emerge, indicating a pressure-induced phase transition. However, all diffraction peaks initially observed in the starting Bi_2NiTiO_6 are still present up to the maximum experimental pressure. Upon decompression to ambient conditions, the sample was recovered with its initial structure, indicating that this phase transition is reversible. Based on Rietveld refinements, all diffraction patterns collected in the pressure range of 0–36.7 GPa can be refined with similar R factors based on the $Pn2_1a$ structure shown in Figure 1. These results show an

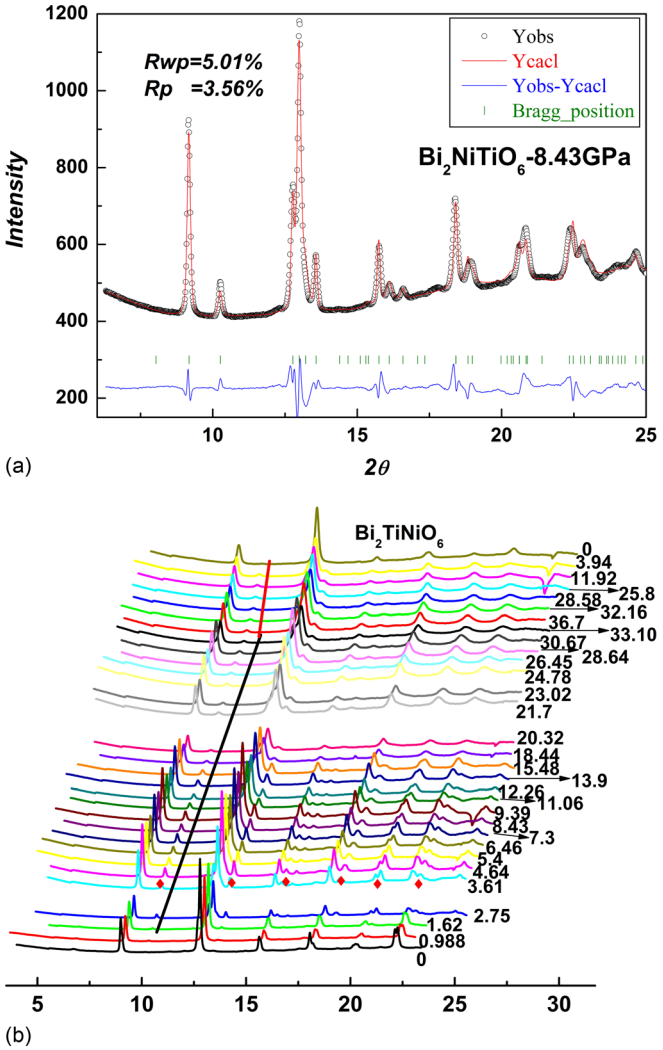

FIG. 4. (a) The refined data of synchrotron X-ray diffraction pattern of Bi_2NiTiO_6 at pressure of 8.43 GPa. (b) AD-XRD collected at BSRF at room temperature in the pressure range from ambient pressure to maximum 36.7 GPa. The straight lines are guide for your eyes, and the dots show the new peaks position when pressure is higher than ~2 GPa.

isostructural phase transition occurred at ~2 GPa, another phase transition at ~15 GPa.

Figure 5(b) shows the pressure dependency of the unit-cell volume for Bi_2NiTiO_6, where the solid lines are the fitting results for two isostructural phases using the second-order Birch equation of state (EOS)[26]

$$P(GPa) = \frac{3}{2} * B_0 * [(V_0/V)^{7/3} - (V_0/V)^{5/3}] * \{1 - (3 - 3 * B_0'/4) * [(V_0/V)^{2/3} - 1]\}. \quad (1)$$

With B_0' fixed at 4, we obtained the ambient isothermal bulk moduli of 94(7) GPa, 145(9) GPa, and 355(10) GPa, respectively, for the three phases. The fitted unit-cell volumes, V_0, of the three phases at ambient conditions are 244.6×10^{-3} nm^3, 244.4×10^{-3} nm^3, and 236.1×10^{-3} nm^3, respectively.

Temperature can also drive phase transitions in ferroelectric phase materials as what pressure can do. We performed *in situ* high-temperature XRD experiments at atmospheric pressure. At temperatures above 823 K, a series of new diffraction peaks appears, and the diffraction pattern is similar to those observed at pressures higher than ~2 GPa, as shown in Figure 5(c). We refined all XRD patterns collected at different temperatures and pressures by using the GSAS program package. Figures 5(a) and 5(d) are the refined X and Z coordinates evolutions of Bi ions under different pressures and at different temperatures, respectively. The evolutions of Ni and Ti cations shifts as a function of high pressure are almost ignorable compared with Bi cation shifts and are not shown here. The pressure dependence of Bi ion positions is not continuous at ~2 GPa and ~15 GPa, corresponding to the two isostructural phase transitions. The temperature dependence of Bi ion positions is not continuous at temperature higher than 823 K. Compared Figures 5(a) and 5(d), we conclude that the phase transition with temperature is identical with the isostructural phase transition at around 15 GPa. In Bi-based multiferroic, the $6s^2$ lone pairs are thought to be the source of ferroelectric polarization. In the case of Bi_2NiTiO_6, it is conceivable based on the findings of this work that there may exist rich physical phenomena to be uncovered at elevated temperature and pressure.

C. Thermal equations of state of Bi_2NiTiO_6

Figures 6 show the relations between unit-cell volumes and pressures at different temperatures for high pressure phase Bi_2NiTiO_6. We employ a modified high-T Birch-Murnaghan EOS,[27–31] truncated to third order, to derive the thermoelastic parameters based on the measured P-V-T data for Bi_2NiTiO_6. A general form of this modified EOS is formulated by

$$P = 3K_T f(1+2f)^{5/2}\left[1 - \frac{3}{2}(4 - K')f + \ldots\right], \quad (2)$$

where

$$K_T = K_{T0} + (\partial K/\partial T)_P(T - 300),$$

$$K' = (\partial K/\partial P)_T,$$

and

$$f = \frac{1}{2}[(V_T/V_{PT})^{2/3} - 1],$$

$$V_T = V_0 \exp\left[\int \alpha(0,T)dT\right].$$

In Eq. (2), K_{T0} and K_T represent the isothermal bulk modulus at 300 K and a higher temperature T, and $(\partial K/\partial T)$ and $(\partial K/\partial P)$ stand for the temperature and pressure derivatives of the bulk modulus, respectively. V_0, V_T, and V_{PT} correspond to the unit-cell volumes at ambient conditions, at ambient pressure and temperature T, and at high P-T conditions, respectively. $\alpha(0,T)$ is the volumetric thermal expansion at atmospheric pressure, typically represented by $\alpha(0,T) = a + bT - c/T^2$ (T in Kelvin, see Ref. 32). In the modified high-T Birch-Murnaghan EOS, the temperature effects are taken into account by replacing K_0 with K_T and substituting V_0/V_P with V_T/V_{PT} in the isothermal EOS.

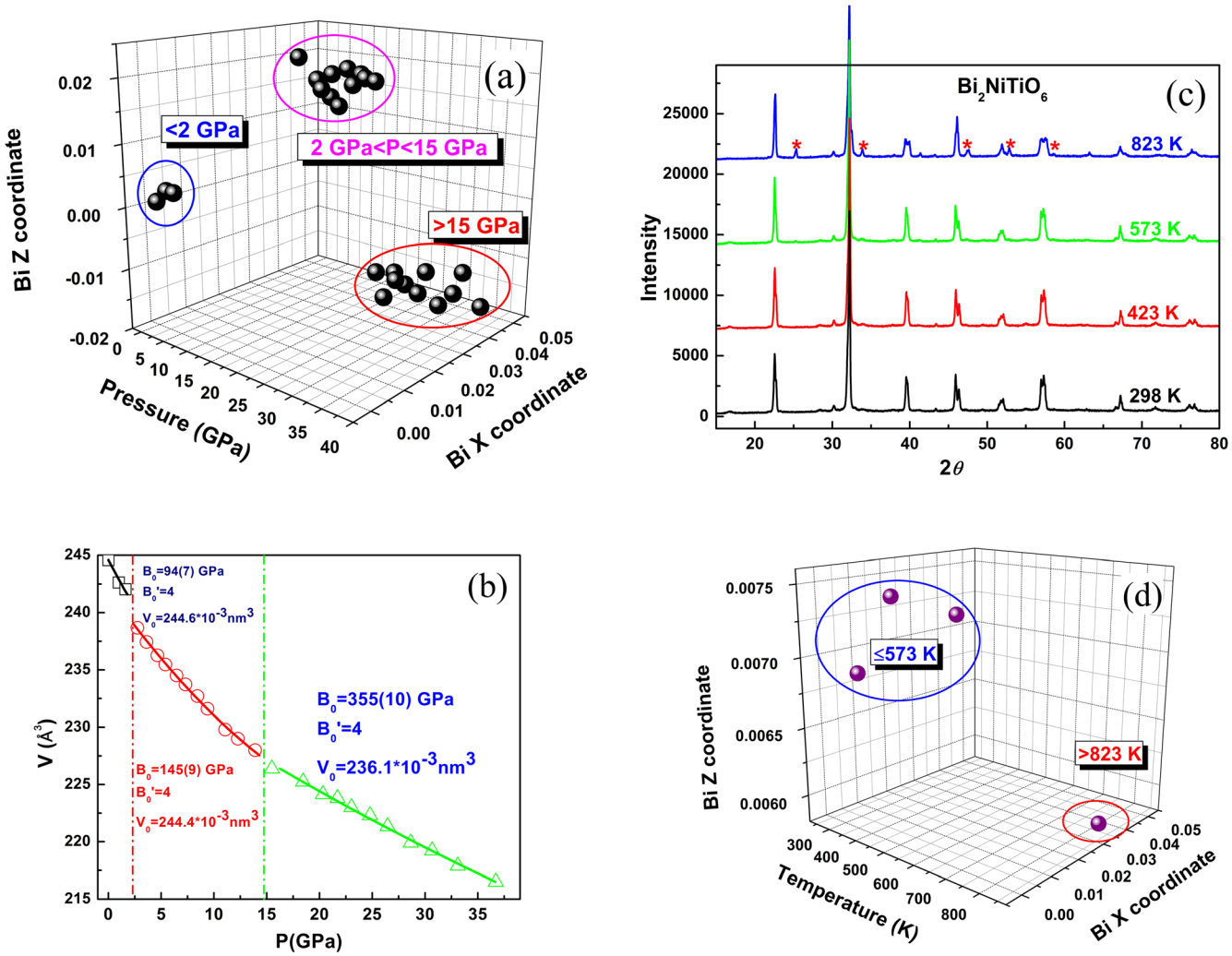

FIG. 5. (a) and (d) are the Bi ion X and Z position variations under different pressures and at different temperatures, respectively. The pressure dependence of Bi ion positions is not continuous at ~2 GPa and ~15 GPa, which is consistent with the unit cell parameters and volume anomalies under pressures and at different temperatures. (b) The volume variation under pressure and the two isostructural phase transitions correspond to the Bi ion position discontinuity. (c) The XRD patterns as a function of temperature up to 823 K. The new peaks emerging temperature is consistent with the Bi ion position discontinuity.

Because of the limited pressure range that restricts an accurate constraint on K', we assume $K'=4$ for Bi_2NiTiO_6 in Eq. (2) throughout the data analysis. Similarly, we ignore the term of c/T^2 in $\alpha(0,T)$ as well as higher-order terms and cross derivatives of the bulk modulus such as ∂^2K/∂^2T and $\partial^2K/\partial P\partial T$. From least-squares fitting of the *P-V-T* data using Eq. (2), we obtain for the orthorhombic Bi_2NiTiO_6, $K_0=115(3)$ GPa, $(\partial K/\partial T)_P=-0.017(7)\,\mathrm{GPa\,K^{-1}}$, and $\alpha(0,T)=a+bT$ with $a=2.1(2)\times10^{-5}\,\mathrm{K^{-1}}$ and $b=2.25\times10^{-8}\,\mathrm{K^{-2}}$. Errors of these thermoelastic parameters were from those of Le Bail profile fitting; uncertainties in the *P-V-T* measurements were not included in the error estimation. For the high pressure orthorhombic Bi_2NiTiO_6, the bulk modulus obtained here (115(3) GPa) is slightly smaller than that fitted from the DAC data at room temperature. Because the presence of deviatoric stress in our DAC experiments, an important factor causing the K_0 discrepancy is the angle between the pressure loading direction and the diffraction plane (φ),[33,34] which is about 90° difference between our cubic anvil apparatus and the conventional DAC setup. In our experimental setup, the diffraction plane is almost perpendicular to the pressure loading direction. Thus the XRD data collected correspond to the maximum stress direction, which would result in smaller bulk modulus if no heating is applied to release the stress.

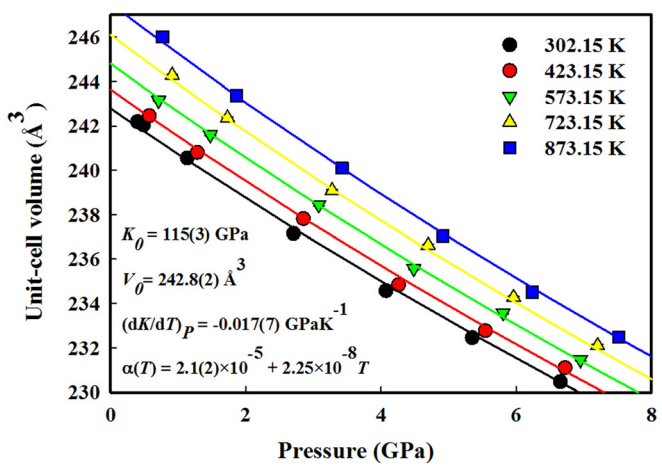

FIG. 6. *P-V-T* data measured for high pressure phase Bi_2NiTiO_6. The curves represent results of the least-squares fitting using Eq. (2).

From the thermodynamic identity,

$$(\partial\alpha/\partial P)_T = (\partial K/\partial T)_P K_{To}^{-2}. \quad (3)$$

The pressure derivatives of the volume thermal expansivity, $(\partial\alpha/\partial P)_T$, are calculated to be $-1.3(6)\times10^{-6}\,K^{-1}\,GPa^{-1}$ for $Bi_2(NiTi)O_6$. The uncertainties in $(\partial\alpha/\partial P)_T$ are estimated from the error propagation of K_{T0} and $(\partial K/\partial T)_P$.

IV. CONCLUSIONS

In conclusion, the high pressure synthesized Bi_2NiTiO_6 multiferroic compound shows a first class ferroelectric phase transition T_C at 513 K while heating and a typical canted-spin interaction with magnetic transition temperature T_M at 58 K with complicated magnetic interactions. High-pressure XRD shows that there are two isostructural phase transitions at ~2 GPa and ~15 GPa, which are caused by the discontinuous movement of Bi iron position. Using second order Birch equation of state, we obtained the ambient pressure isothermal bulk modulus $B_0 = 94(7)$ GPa, 145(9) GPa, and 355(10) GPa for the three phases, respectively. With increasing temperature, there is also an isostructural phase transition at temperature higher than 823 K, which corresponds to the one occurred at ~15 GPa. High-T EOS has been applied to derive thermal equations of state for high pressure phase Bi_2NiTiO_6, which includes temperature and pressure derivatives of thermal expansion and elastic bulk modulus. Other thermoelastic parameters for high pressure phase Bi_2NiTiO_6 has been determined for the first time. These results extend our knowledge of the fundamental properties of high pressure phase Bi_2NiTiO_6 and provide basic parameters for modeling thermal-mechanical behavior of perovskite-type multiferroic materials.

ACKNOWLEDGMENTS

This work was supported by the laboratory-directed research and development (LDRD) program of Los Alamos National Laboratory, which is operated by Los Alamos National Security LLC under DOE Contract No. DE-AC52-06NA25396. Use of the National Synchrotron Light Source, Brookhaven National Laboratory was supported by the U.S. Department of Energy, Office of Science, Office of Basic Energy Sciences, under Contract No. DE-AC02-98CH10886. Use of the X17B2 beamline was supported by COMPRES, the Consortium for Materials Properties Research in Earth Sciences under NSF Cooperative Agreement No. EAR 01-35554, and by the Mineral Physics Institute, Stony Brook University. Work at IOPCAS was supported by NSF & MOST of China through research projects (Nos. 2009CB623301 and 10820101049).

[1]G. A. Smolenskii and V. A. Bokov, J. Appl. Phys. **35**, 915 (1964).
[2]W. Qu, X. Tan, R. W. McCallum, D. P. Cann, and E. Ustundag, J. Phys.: Condens. Matter **18**, 8935 (2006).
[3]T. Kimura, T. Goto, H. Shintani, K. Ishizaka, T. Arima, and Y. Tokura, Nature (London) **426**, 55 (2003).
[4]N. Hur, S. Park, P. A. Sharma, J. S. Ahn, S. Guha, and S.-W. Cheong, Nature (London) **429**, 392 (2004).
[5]N. A. Hill, J. Phys. Chem. B **104**, 6694 (2000).
[6]N. A. Hill and A. Filippetti, J. Magn. Magn. Mater. **242–245**, 976 (2002).
[7]M. Azuma, K. Takata, T. Saito, S. Ishiwata, Y. Shimakawa, and M. Takano, J. Am. Chem. Soc. **127**, 8889 (2005).
[8]H. Hughes, M. M. B. Allix, C. A. Bridges, J. B. Claridge, X. Kuang, H. Niu, S. Taylor, W. Song, and M. J. Rosseinsky, J. Am. Chem. Soc. **127**, 13790 (2005).
[9]R. Seshadri and N. A. Hill, Chem. Mater. **13**, 2892 (2001).
[10]N. A. Hill and K. M. Rabe, Phys. Rev. B **59**, 8759 (1999).
[11]E. Montanari, L. Righi, G. Calestani, A. Migliori, E. Gilioli, and F. Bolzoni, Chem. Mater. **17**, 1765 (2005).
[12]T. Kimura, S. Kawamoto, I. Yamada, M. Azuma, M. Takano, and Y. Tokura, Phys. Rev. B **67**, 180401(R) (2003).
[13]T. Atou, H. Chiba, K. Ohoyama, Y. Yamaguchi, and Y. Syono, J. Solid State Chem. **145**, 639 (1999).
[14]A. M. dos Santos, A. K. Cheetham, T. Atou, Y. Syono, Y. Yamaguchi, K. Ohoyama, H. Chiba, and C. N. R. Rao, Phys. Rev. B **66**, 064425 (2002).
[15]A. Sharan, J. Lettieri, Y. Jia, W. Tian, X. Pan, D. G. Schlom, and V. Gopalan, Phys. Rev. B **69**, 214109 (2004).
[16]J. M. Moreau, C. Michel, R. Gerson, and W. J. James, J. Phys. Chem. Solids **32**, 1315 (1971).
[17]J. B. Neaton, C. Ederer, U. V. Waghmare, N. A. Spaldin, and K. M. Rabe, Phys. Rev. B **71**, 014113 (2005) and references therein.
[18]R. Cohen, Nature (London) **358**, 136 (1992).
[19]Y. Inaguma and T. Katsumata, Ferroelectrics **286**, 111 (2003).
[20]K. Kitada, M. Kobune, W. Adachi, T. Yazawa, H. Saitoh, K. Aoki, J. Mizuki, K. Ishikawa, Y. Hiranaga, and Y. Cho, Chem. Lett. **37**, 560 (2008).
[21]K. Fukushima, M. Koboune, T. Yamaji, H. Tada, A. Mineshige, T. Yazawa, H. Fujisawa, M. Shimizu, Y. Nishhata, J. Mizuki, H. Yamaguchi, and K. Honda, Jpn. J. Appl. Phys. **46**, 6938 (2007).
[22]M. R. Palacin, J. Bassas, J. Rodriguez-Carvajal, and P. Gomez-Romero, J. Mater. Chem. **3**, 1171 (1993).
[23]H. K. Mao, J. A. Xu, and P. M. Bell, J. Geophys. Res. **91**, 4673, doi:10.1029/JB091iB05p04673 (1986).
[24]D. J. Weidner, M. T. Vaughan, J. Ko, Y. Wang, X. Liu, A. Yeganeh-haeri, R. E. Pacalo, and Y. Zhao, in *High-Pressure Research: Application to Earth and Planetary Sciences*, edited by Y. Syono and M. H. Manghnani (American Geophysics Union, Washington, DC, 1992), p. 13.
[25]A. C. Larson and R. B. Von Dreele, "General structure analysis system (GSAS)," Los Alamos National Laboratory Report LAUR, 2004, pp. 86–748.
[26]F. Birch, Phys. Rev. **71**, 809 (1947).
[27]F. D. Murnaghan, Am. J. Math. **59**, 235 (1937).
[28]S. K. Saxena and J. Zhang, Phys. Chem. Miner. **17**, 45 (1990).
[29]Y. Zhao, D. Schiferl, and T. J. Shankland, Phys. Chem. Miner. **22**, 393 (1995).
[30]Y. Zhao, A. C. Lawson, J. Zhang, B. I. Bennett, and R. B. Von Dreele, Phys. Rev. B **62**, 8766 (2000).
[31]Y. J. Wang, J. Z. Zhang, L. L. Daemen, Z. J. Lin, and Y. S. Zhao, Phys. Rev. B **78**, 224106 (2008).
[32]I. Suzuki, J. Phys. Earth **23**, 145 (1975).
[33]J. Zhang, I. Martinez, F. Guyot, P. Gillet, and S. K. Saxena, Phys. Chem. Miner. **24**, 122 (1997).
[34]H. N. Dong, D. W. He, and T. S. Duffy, Phys. Rev. B **79**, 014105 (2009).